Relativistic effects and angular dependence in the reaction $\bar{p}p \to \pi^-\pi^+$

B. El-Bennich* and W. M. Kloet
Department of Physics and Astronomy, Rutgers University, 136 Frelinghuysen Road, Piscataway, New Jersey 08854-8019, USA
(Received 23 March 2004; published 15 September 2004)

We present a fit to the low energy antiproton ring at CERN data on $\bar{p}p \to \pi^-\pi^+$ differential cross sections and analyzing powers motivated by relativistic considerations. Within a quark model describing this annihilation, we argue, since the pions are highly energetic, that relativistic effects cannot be neglected. The intrinsic pion wave functions are Lorentz transformed to the center-of-mass frame. This change in quark geometry gives rise to additional angular dependence in the transition operators and results in a relative enhancement of higher $J \geqslant 2$ partial wave amplitudes. The fit to the data is improved significantly.

DOI: 10.1103/PhysRevC.70.034002 PACS number(s): 13.75.Cs, 12.39.Jh, 21.30.Fe, 25.43.+t

I. INTRODUCTION

We recently studied effects of particle size and final-state interactions in the reaction $\bar{p}p \to \pi^-\pi^+$ within the framework of a constituent quark model [1]. The aim was to improve previous attempts [2,3] to describe the low energy antiproton ring at CERN (LEAR) data on $\bar{p}p \to \pi^-\pi^+$ differential cross sections $d\sigma/d\Omega$ and analyzing powers A_{0n} in the momentum range from 360–1550 MeV/c [4]. As of yet, theoretical approaches, whether using a baryonic or a quark picture [3,5–7,9,10], have not been successful in reproducing the characteristic double-dip structure of the A_{0n} observables nor the $d\sigma/d\Omega$ forward peaks at low momenta. The large variations of the LEAR observables as a function of the angle portends the presence of a substantial number of partial wave amplitudes already at low energies. In fact, the experimental data on differential cross sections, as well as those on asymmetries point to a significant $J=2$, $J=3$, and even higher J contributions [11–14]. Model calculations [3,5–7,9,10], however, nearly always lead to scattering amplitudes which are strongly dominated by total angular momentum $J=0$ and $J=1$. This is due to a rather short range of the annihilation mechanism in these models.

In order to study possible higher partial wave $J \geqslant 2$ contributions, the role of final-state $\pi\pi$ interactions has been investigated in Ref. [1,6–8]. For example, in Ref. [1] we made use of the nonplanar $R2$ quark-flow diagrams, in which a $\bar{q}q$ pair in either a $^3S_1$ or a $^3P_0$ state is annihilated and momentum is transferred to a remaining quark or antiquark as discussed in Refs. [2,3]. Switching on the $\pi\pi$ interaction moderately improved the fit of A_{0n}, in particular the double-dip structure at low momenta is slightly more pronounced. This is caused by a readjustment of the strengths of the helicity amplitudes of different total angular momentum J. Nonetheless, the predictions for $d\sigma/d\Omega$ showed only a modest improvement over the model without final-state interactions.

The main improvement obtained in Ref. [1], however, is due to a different aspect, namely a readjustment of the size parameters of the intrinsic proton and pion wave functions, so that the radii of the proton, antiproton, and pions increase. In a final fit these radii are larger by about 7% than the respective measured charge distribution radii. This runs contrary to the view that the valence quarks occupy a smaller volume than indicated by the charge radii. Nevertheless, introducing larger radii as well as final-state interactions, improves the quality of the fit in Ref. [1] dramatically—the forward and backward peaks of $d\sigma/d\Omega$ are very well reproduced and so are the characteristic double-dip structures of A_{0n}. It should come as no surprise that the relative contribution of the higher $J \geqslant 2$ amplitudes in Ref. [1] turns out to be significantly larger than in Ref. [3].

In this paper, we report an alternative approach that also leads to enhancement of the higher partial waves. It addresses the relativistic effects due to Lorentz transformed intrinsic pion wave functions in the reaction $\bar{p}p \to \pi^-\pi^+$. The reason for this rather different approach stems from the observation that at the center-of-mass (c.m.) energies $\sqrt{s}$ considered in the LEAR experiment $\bar{p}p \to \pi^-\pi^+$, the produced pions are highly energetic. The relativistic factor in this energy range is $\gamma = E_{\rm cm}/2m_\pi c^2 \simeq 6.8-8.0$, which means the pions are ejected at speeds $v \simeq 0.98c$. One therefore expects considerable relativistic effects due to their modified internal structure. In the c.m. frame, in which the transition amplitudes are calculated, the intrinsic pion wave functions employed must be Lorentz transformed from the pion rest frame. In our model [1–3], the intrinsic pion as well as the proton and antiproton wave functions are of Gaussian form in their respective rest frames. We neglect the distortions of the proton and antiproton intrinsic wave function due to their much smaller kinetic energy and larger mass.

The relativistic effects have several consequences. First, the intrinsic geometry of the pions is modified—instead of spherical particles one deals now with highly flattened ellipsoids in the c.m. frame. Obviously, the reaction geometry is altered also, since the boosted pion wave functions enter the computation of the transition operators, which are obtained from an overlap integral of initial antiproton-proton, final pion-pion wave functions, and the $^3S_1$ or $^3P_0$ annihilation mechanism. Details of this calculation were presented in Ref. [15]. Secondly, due to less overlap of the pion and antiproton-proton intrinsic wave functions, the annihilation range *actually* decreases, but this effect is far from isotropic.

*Electronic address: bennich@physics.rutgers.edu

As a result, the transition operators exhibit significant additional angle dependence. Finally, the annihilation amplitudes, already nonlocal in the case of nonrelativistic wave functions, become explicitly dependent on the c.m. energy $\sqrt{s}$ via the boost factor γ.

In Ref. [15] it was shown that the relativistic transformation of the spatial part of the intrinsic pion wave functions introduces additional angle-dependent terms in the transition operators. These terms also depend on the boost factor γ. In this paper, we present a fit to the LEAR data on $\bar{p}p \to \pi^-\pi^+$ using the $R2$ transition operators of Ref. [15], which supports our claim that relativistic considerations lead to a strongly modified angular momentum content of the helicity amplitudes for $0 \leqslant J \leqslant 4$. Especially the amplitudes for $J \geqslant 2$ are enhanced considerably. Even though we keep the original particle radii as in Refs. [2,3] dictated by the quark model, which are smaller than the corresponding charge distribution radii, we achieve a very good reproduction of the LEAR observables $d\sigma/d\Omega$ and A_{0n}, comparable to the one in Ref. [1].

II. RELATIVISTIC MODIFICATIONS

We summarize the effects of Lorentz transforming intrinsic pion wave functions on $\bar{p}p \to \pi^-\pi^+$ annihilation operators within the constituent quark model. The actual details may be found in Ref. [15]. In the pion rest frame, the radial part of its intrinsic wave function is described by a Gaussian of the form

$$\psi_\pi(\mathbf{r}_q, \mathbf{r}_{\bar{q}}) = N_\pi \exp\left\{ -\frac{\beta}{2} \sum_{i=q,\bar{q}} (\mathbf{r}_i - \mathbf{R}_\pi)^2 \right\}, \tag{1}$$

which reads in the c.m. frame

$$\psi_\pi(l^{-1}\mathbf{r}_q, l^{-1}\mathbf{r}_{\bar{q}}) = \tilde{N}_\pi \exp\left\{ -\frac{\beta}{2} \sum_{i=q,\bar{q}} [(\mathbf{r}_i - \mathbf{R}_\pi)_\perp^2 + \gamma^2 (\mathbf{r}_i - \mathbf{R}_\pi)_\parallel^2] \right\}. \tag{2}$$

The vectors $\mathbf{r}_q$ and $\mathbf{r}_{\bar{q}}$ are the quark and antiquark coordinates, $\mathbf{R}_\pi = \frac{1}{2}(\mathbf{r}_q + \mathbf{r}_{\bar{q}})$ is the pion coordinate, and β is the size parameter. As mentioned above, in previous work [1] we varied the value of β in order to obtain an increase in the annihilation range. In this paper we use throughout the fixed value $\beta = 3.23$ fm^{-2}, which corresponds to a pion radius of 0.48 fm [2,3,16]. The normalization factor $\tilde{N}_\pi = \sqrt{\gamma} N_\pi$ is due to the condition that ψ_π be normalized to unity in the c.m.

The c.m. wave functions of Eq. (2) are used to compute the transition operators for the $^3P_0$ and $^3S_1$ annihilation amplitudes. It is shown in Ref. [15] that these operators acquire new terms if compared with the nonrelativistic expressions [2] and which manifestly introduce additional angular dependence. We here briefly recapitulate the results for the $R2$ diagrams from Ref. [15]. The complete form of the $R2$ transition operators for the vacuum $^3P_0$ amplitude is

$$\begin{aligned} \hat{T}(^3P_0) = i\mathcal{N}[&A_V \boldsymbol{\sigma}\cdot\mathbf{R}' \sinh(C\mathbf{R}\cdot\mathbf{R}') \\ &+ B_V \boldsymbol{\sigma}\cdot\mathbf{R} \cosh(C\mathbf{R}\cdot\mathbf{R}') \\ &+ C_V(\boldsymbol{\sigma}\cdot\hat{\mathbf{R}}')R\cos\theta\cosh(C\mathbf{R}\cdot\mathbf{R}')]\exp\{A\mathbf{R}'^2 \\ &+ B\mathbf{R}^2 + D\mathbf{R}^2\cos^2\theta\}. \end{aligned} \tag{3}$$

The total $^3S_1$ amplitude for the longitudinal component is given by

$$\begin{aligned} \hat{T}(^3S_1^L) = i\mathcal{N}[&A_L \boldsymbol{\sigma}\cdot\mathbf{R}' \sinh(C\mathbf{R}\cdot\mathbf{R}') \\ &+ B_L \boldsymbol{\sigma}\cdot\mathbf{R} \cosh(C\mathbf{R}\cdot\mathbf{R}') \\ &+ C_L(\boldsymbol{\sigma}\cdot\hat{\mathbf{R}}')R\cos\theta\cosh(C\mathbf{R}\cdot\mathbf{R}')]\exp\{A\mathbf{R}'^2 \\ &+ B\mathbf{R}^2 + D\mathbf{R}^2\cos^2\theta\} \end{aligned} \tag{4}$$

and

$$\begin{aligned} \hat{T}(^3S_1^T) = \mathcal{N}[&A_T \boldsymbol{\sigma}\cdot\mathbf{R}' \cosh(C\mathbf{R}\cdot\mathbf{R}') \\ &+ B_T \boldsymbol{\sigma}\cdot\mathbf{R} \sinh(C\mathbf{R}\cdot\mathbf{R}') \\ &+ C_T(\boldsymbol{\sigma}\cdot\hat{\mathbf{R}}')R\cos\theta\sinh(C\mathbf{R}\cdot\mathbf{R}')]\exp\{A\mathbf{R}'^2 \\ &+ B\mathbf{R}^2 + D\mathbf{R}^2\cos^2\theta\} \end{aligned} \tag{5}$$

for the transversal component. The factor $\mathcal{N}$ is an overall normalization and $\mathbf{R}' = \mathbf{R}_{\pi^-} - \mathbf{R}_{\pi^+}$ and $\mathbf{R} = \mathbf{R}_{\bar{p}} - \mathbf{R}_p$ are the relative $\pi^-\pi^+$ and antiproton-proton coordinates, respectively. The angle θ is between $\mathbf{R}'$ and $\mathbf{R}$ in the c.m. frame. In the experiment it is the c.m. angle between the antiproton beam direction and the outgoing π^- direction. The new terms mentioned previously are C_V, C_L, C_T, and D. The selection rules for the $R2$ diagrams discussed in Ref. [2] are unchanged. More precisely, $\hat{T}(^3P_0)$ and $\hat{T}(^3S_1^L)$ act in $\bar{p}p$ states with $J^\pi = 0^+, 2^+, 4^+, \ldots$ waves while $\hat{T}(^3S_1^T)$ contributes only to $J^\pi = 1^-, 3^-, 5^-, \ldots$ waves. The explicit expressions for the coefficients of Eqs. (3)–(5) are [with $\alpha = 2.80$ fm^{-2} being the proton size parameter [15] defined similarly to the pion size parameter $\beta = 3.23$ fm^{-2} of Eq. (1)]

$$A = -\frac{\alpha(5\alpha + 4\beta\gamma^2)}{2(4\alpha + 3\beta\gamma^2)}, \tag{6}$$

$$B = -\frac{3(7\alpha^2 + 18\alpha\beta\gamma^2 + 9\beta^2\gamma^4)}{8(4\alpha + 3\beta\gamma^2)} - D, \tag{7}$$

$$C = -\frac{3\alpha(\alpha + \beta\gamma^2)}{2(4\alpha + 3\beta\gamma^2)}, \tag{8}$$

$$D = -\frac{9\beta(\gamma^2 - 1)}{8}\left\{ 1 + \frac{\alpha^2}{(5\alpha + 4\beta)(5\alpha + 4\beta\gamma^2)} \right\}, \tag{9}$$

$$A_V = \frac{\alpha(\alpha + \beta\gamma^2)}{4\alpha + 3\beta\gamma^2}, \tag{10}$$

$$B_V = \frac{3(\alpha + \beta\gamma^2)(5\alpha + 3\beta\gamma^2)}{2(4\alpha + 3\beta\gamma^2)} - C_V, \tag{11}$$

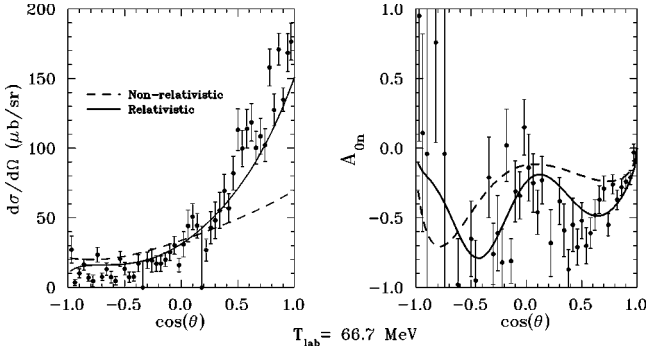

FIG. 1. Differential cross section and analyzing power of the reaction $\bar{p}p \to \pi^-\pi^+$ at $T_{\rm lab}=66.7$ MeV ($p_{\rm lab}=360$ MeV/c). Experimental data are from Hasan *et al.* [4]. Solid curves denote quark model predictions with boosted intrinsic pion wave functions; dashed lines represent predictions with original (spherical) pion wave functions.

$$C_V = \frac{3\beta(\gamma^2-1)}{2}\left\{1+\frac{\alpha^2}{(5\alpha+4\beta)(5\alpha+4\beta\gamma^2)}\right\}, \quad (12)$$

$$A_L = -A_V, \quad (13)$$

$$B_L = \frac{9(\alpha+\beta\gamma^2)^2}{2(4\alpha+3\beta\gamma^2)} - C_L, \quad (14)$$

$$C_L = \frac{3\beta(\gamma^2-1)}{2}\left\{1-\frac{\alpha^2}{(5\alpha+4\beta)(5\alpha+4\beta\gamma^2)}\right\}, \quad (15)$$

$$A_T = -2A_V, \quad (16)$$

$$B_T = \frac{3\alpha(\alpha+\beta\gamma^2)}{4\alpha+3\beta\gamma^2} - C_T, \quad (17)$$

$$C_T = -\frac{3\beta\alpha^2(\gamma^2-1)}{(5\alpha+4\beta)(5\alpha+4\beta\gamma^2)}. \quad (18)$$

Clearly, C_V, C_L, C_T, and D vanish in the nonrelativistic limit $\gamma \to 1$. A noticeable feature is that some of the new coefficients become relatively large for large γ values. In particular, the $DR^2\cos^2\theta$ term dominates the exponential part of Eqs. (3)–(5) and, for example, $C_V \gg A_V, B_V$ and $C_L \gg A_L, B_L$. On the other hand, one finds that $C_T \simeq A_T \simeq B_T$.

At this stage, we will neglect additional relativistic corrections due to the (anti)quark spinors in the final-state pions, since it was argued in Ref. [15] that the boosting of spin wave functions results in relatively smaller corrections.

III. RESULTS

The LEAR data for the $d\sigma/d\Omega$ and A_{0n} have been fitted using the transition operators in Eqs. (3)–(5). As before, taking only the $R2$ topology into account, we use a distorted wave approximation (DWA)

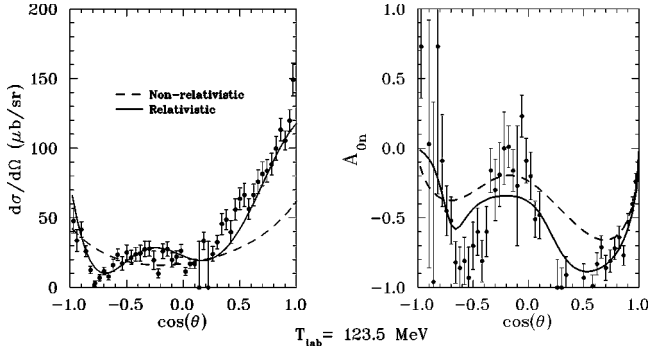

FIG. 2. As in Fig. 1 but for $T_{\rm lab}=123.5$ MeV ($p_{\rm lab}=497$ MeV/c).

$$T^J = \int d\mathbf{R}\, d\mathbf{R}'\, \phi^J_{\pi\pi}(\mathbf{R}')\hat{T}_{R2}(\mathbf{R},\mathbf{R}')\Psi^{J,l=J\pm1}_{\bar{p}p}(\mathbf{R}) \quad (19)$$

to obtain the scattering matrix elements and introduce final-state interactions as in Ref. [1]. The pion wave function $\phi^J_{\pi\pi}(\mathbf{R}')$ is obtained from the coupled-channel model of Ref. [17] and can be parametrized with phases δ_J and inelasticities η_J. The initial $\bar{p}p$ wave function $\Psi^{J,l=J\pm1}_{\bar{p}p}(\mathbf{R})$ is taken from an optical potential model [18]. Both $\phi^J_{\pi\pi}(\mathbf{R}')$ and $\Psi^{J,l=J\pm1}_{\bar{p}p}(\mathbf{R})$ still contain the angle dependence appropriate for the values of J and l.

We select from the specific energies where LEAR data are available [4] the same set of five energies as in Ref. [1]: $T_{\rm lab}=66.7$, 123.5, 219.9, 499.2, and 803.1 MeV corresponding to antiproton momenta of, respectively, $p_{\rm lab}=360$, 497, 679, 1089, and 1467 MeV/c. $T_{\rm lab}$ is the laboratory kinetic energy of the antiproton beam. In fitting the data, we proceed as in Ref. [1]. One starts with $\pi^-\pi^+$ final-state plane waves, i.e., with $\delta_J=0$ and $\eta_J=1$, and varies these parameters for $0 \leqslant J \leqslant 4$. The other parameters are the relative (complex) strength λ as defined by the $R2$ transition amplitude

$$\hat{T}_{\rm tot.}(\mathbf{R}',\mathbf{R}) = N_0\left[\hat{T}\left({}^3P_0\right)(\mathbf{R}',\mathbf{R}) + \lambda\hat{T}\left({}^3S_1\right)(\mathbf{R}',\mathbf{R})\right], \quad (20)$$

and the overall normalization N_0. The size parameters α and β of the quark model are kept fixed at the original values $\alpha=2.8$ fm^{-2} and $\beta=3.23$ fm^{-2} [2,3,16]. The aim is to find

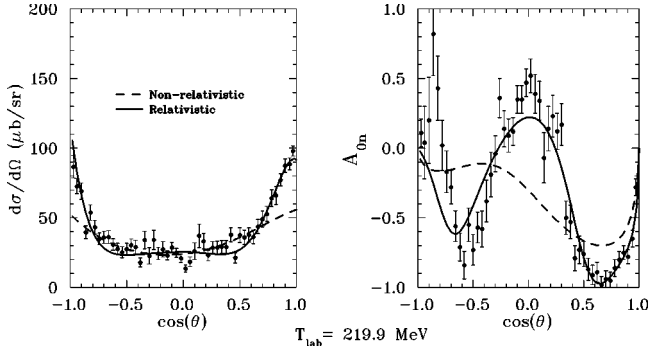

FIG. 3. As in Fig. 1 but for $T_{\rm lab}=219.9$ MeV ($p_{\rm lab}=679$ MeV/c).

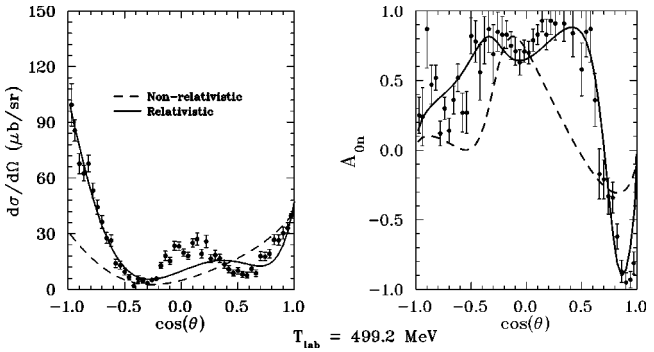

FIG. 4. As in Fig. 1 but for $T_{\rm lab}=499.2$ MeV ($p_{\rm lab}=1089$ MeV/c).

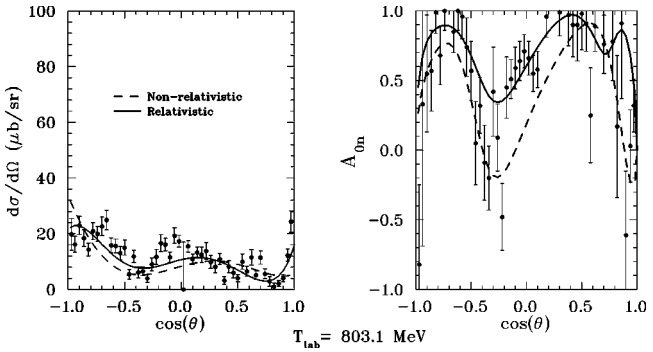

FIG. 5. As in Fig. 1 but for $T_{\rm lab}=803.1$ MeV ($p_{\rm lab}=1467$ MeV/c).

out how much improvement is obtained solely from introducing final-state interactions.

At this initial stage, no relativistic effects have been included which implies $\gamma=1$. The results of this fit are plotted in Figs. 1–5 as dashed lines. They will serve as reference points and were obtained previously in Ref. [1], where the model with and without final-state interactions was discussed. It was found that the improvement from just final-state interactions is very modest—the double-dip structure in the analyzing power is somewhat more enhanced but the forward peaks in the differential cross sections at $T_{\rm lab}=66.7$ and 123.5 MeV ($p_{\rm lab}=360$ and 497 MeV/c) as well as the backward peaks at $T_{\rm lab}=499.2$ and 803.1 MeV ($p_{\rm lab}=1089$ and 1467 MeV/c) are poorly reproduced.

Next, we consider the effects of relativistic distortions of the intrinsic pion wave functions. Hence, the transition operators of Eqs. (3)–(5) must be used. The exponential part is dominated by the D term (typically $D\simeq 200$ fm^{-2}, about two orders of magnitude larger than the C term), which makes the partial wave amplitudes T^J very sensitive to the value of the relative strength $\lambda=|\lambda|\exp(i\theta_\lambda)$ of the $^3S_1$ versus the $^3P_0$ mechanism and to the pion wave parameters η_J and δ_J. This is a consequence of the strong angle dependence of $\exp\{DR^2\cos^2\theta\}$. In order for the partial wave expansion of the scattering amplitude T to converge, all ingredients must be fine tuned, in particular the phases δ_J and inelasticities η_J for $0\leqslant J\leqslant 4$. It should be emphasized that α and β remain fixed.

The resulting fit is illustrated in Figs. 1–5, where the predictions that include relativistic effects and final-state interactions are presented as solid curves. This fit is a significant improvement over the nonrelativistic version of the $R2$ annihilation model (dashed curve). The differential cross sections $d\sigma/d\Omega$ are particularly well reproduced for the energies $T_{\rm lab}=66.7$, 123.5, and 219.9 MeV ($p_{\rm lab}=360$, 497, and 679 MeV/c). For $T_{\rm lab}=499.2$ and 803.1 MeV ($p_{\rm lab}=1089$ and 1467 MeV/c), the results for $d\sigma/d\Omega$ show improvement in forward and backward directions. At the two higher energies, the experimental double-well structure of the cross section is reproduced, but some problems remain near $\theta=\pi/2$.

As for the analyzing powers A_{0n}, we are able to describe their double-dip structure, already present in the LEAR data at the lowest energies. At $T_{\rm lab}=219.9$ and 499.2 MeV, where the experimental errors are small, the A_{0n} fit is particularly successful. At the lowest energy, $T_{\rm lab}=66.7$ MeV, the error bars in A_{0n} are rather large and we do not fit very well certain data points. Overall, the improvement over the nonrelativistic treatment is striking. The presented fits are of similar quality to those of Ref. [1], which were obtained for undistorted spherical pions but increased particle radii. Taking into account the relativistic internal distortion of the final mesons therefore offers an interesting alternative.

In Table I, we give the values of the quark model parameters as a function of $T_{\rm lab}$ while the $\pi\pi$ phases δ_J and inelasticities η_J are conveniently listed as a function of c.m. energy $\sqrt{s}$ in Table II. In the quark model parameters of Table I, one notes that the relative strength $|\lambda|$ of the $^3S_1$ versus the $^3P_0$ mechanism still varies with energy but much less so than in the nonrelativistic approach of Ref. [1], which is encouraging. The average value is $|\lambda|\simeq 1.17$. The energy variation of the inelasticities η_J in the $\pi\pi$ interaction observed in Table II may be associated with the presence of $\pi\pi$ resonances, in particular with the f_2 at 2010 MeV in the $J=2$ amplitude.

IV. SUMMARY AND CONCLUSION

We present a fit to the LEAR $\bar{p}p\to\pi^-\pi^+$ data based on relativistic effects in the annihilation. These effects are due

TABLE I. Quark Model parameters as function of $T_{\rm lab}$.

$T_{\rm lab}$ [MeV]	66.7	123.5	219.9	499.2	803.1
$p_{\rm lab}$ [MeV/c]	369	497	679	1089	1467
$\gamma=\sqrt{s}/2m_\pi c^2$	6.841	6.940	7.106	7.564	8.033
$\lvert\lambda\rvert$	1.165	0.889	1.090	1.377	1.320
$\theta_\lambda[^\circ]$	154.51	149.13	82.57	184.14	184.76
N_0 [10^5]	2.999	3.061	3.068	1.739	4.999

TABLE II. Phases shifts δ_J and inelasticities η_J of the final-state $\pi\pi$ interaction for $0 \leqslant J \leqslant 4$ as function of $\sqrt{s}$.

$T_{\rm lab}$ [MeV]	66.7	123.5	219.9	499.2	803.1
$\sqrt{s}$ [MeV]	1910.	1937.	1983.	2111.	2242.
η_0	1.00	0.716	0.811	1.00	1.00
δ_0	67.00	54.37	41.42	−1.704	−17.15
η_1	1.00	0.583	0.666	0.999	1.00
δ_1	43.68	37.11	42.62	−31.62	21.56
η_2	0.968	0.973	0.992	0.538	0.624
δ_2	−17.06	−16.55	−18.78	−37.34	−13.51
η_3	1.00	0.923	1.00	0.946	1.00
δ_3	−11.93	−13.80	−16.07	−6.873	−11.91
η_4	1.00	1.00	1.00	0.946	1.00
δ_4	−0.03	−0.03	−0.04	−0.038	−0.07

to Lorentz transformations of intrinsic pion wave functions from the pion rest frame to the c.m. frame of the reaction. The impact from the modified geometry of the pions is considerable and carries with it a much richer angle dependence of the transition operators.

The quality of this relativistic fit is very similar to the one of a previous fit [1]. However, the approaches are very different. While in Ref. [1] we achieved a good fit by means of particle radii increase, so the antiquarks and quarks do overlap more, in this work we keep the original particle sizes fixed but take into account the relativistic distortions of the pions in the c.m. frame of the reaction.

We conclude that even though observed data at LEAR on $d\sigma/d\Omega$ and A_{0n} indicate strongly the presence of higher partial wave amplitudes, and therefore seem to call for an increase of the annihilation range, one can obtain a similar improvement by additional angle dependence in the transition operators. This additional angle dependence arises naturally when boosted intrinsic pion wave functions are employed in the quark model calculations, as becomes clear from the present fit. Relativistic effects in the reaction $\bar{p}p \rightarrow \pi^-\pi^+$, therefore, should not be ignored.

[1] B. El-Bennich, W. M. Kloet, and B. Loiseau, Phys. Rev. C **68**, 014003 (2003).
[2] G. Bathas and W. M. Kloet, Phys. Lett. B **301**, 155 (1993).
[3] G. Bathas and W. M. Kloet, Phys. Rev. C **47**, 2207 (1993).
[4] A. Hasan *et al.*, Nucl. Phys. **B378**, 3 (1992).
[5] B. Moussallam, Nucl. Phys. **A407**, 413 (1983); *ibid.* **A429**, 429 (1984).
[6] V. Mull, J. Haidenbauer, T. Hippchen, and K. Holinde, Phys. Rev. C **44**, 1337 (1991).
[7] V. Mull, K. Holinde, and J. Speth, Phys. Lett. B **275**, 12 (1992).
[8] A. M. Green and G. Q. Liu, Nucl. Phys. **A486**, 581 (1988).
[9] A. Muhm, T. Gutsche, R. Thierauf, Y. Yan, and Amand Faessler, Nucl. Phys. **A598**, 285 (1996).
[10] Y. Yan and R. Tegen, Phys. Rev. C **54**, 1441 (1996); Nucl. Phys. **A648**, 89 (1999).
[11] M. N. Oakden and M. R. Pennington, Nucl. Phys. **A574**, 731 (1994).
[12] A. Hasan and D. V. Bugg, Phys. Lett. B **334**, 215 (1994).
[13] W. M. Kloet and F. Myhrer, Phys. Rev. D **53**, 6120 (1996).
[14] B. R. Martin and G. C. Oades, Phys. Rev. C **56**, 1114 (1997); *ibid.* **57**, 3492 (1998).
[15] B. El-Bennich and W. M. Kloet, nucl-th/0403050.
[16] A. M. Green and J. A. Niskanen, Nucl. Phys. **A412**, 448 (1984); *ibid.* **A430**, 605 (1984); Mod. Phys. Lett. A **1**, 441 (1986).
[17] W. M. Kloet and B. Loiseau, Eur. Phys. J. A **1**, 337 (1998).
[18] B. El-Bennich, M. Lacombe, B. Loiseau, and R. Vinh Mau, Phys. Rev. C **59**, 2313 (1999).